Immunological control by PARP inhibitors for successful immunotherapy of ovarian carcinoma

Holicek P[1,2], Vosahlikova S[1], Moserova I[1], Orsulic S[3], Mikyskova R[4], Hensler M[1], Kasikova L[1], Lanickova T[1], Novotny O[4], Reinis M[4], Drozenova J[5], Ryska A[6], Laco J[6], Rob L[7], Michal J. Halaska[7], Cibula D[8], Spisek R[1,2], Fucikova J[1,2]

[1]SOTIO Biotech, Prague, Czech Republic; [2]Department of Immunology, Charles University, 2nd Faculty of Medicine and University Hospital Motol, Prague, Czech Republic; [3]Department of Obstetrics and Gynecology, David Geffen School of Medicine, University of California, Los Angeles, CA 90095, USA; VA Greater Los Angeles Healthcare System, Los Angeles, CA 90073, USA; [4]Laboratory of Immunological and Tumour Models, Institute of Molecular Genetics of the Czech Academy of Sciences, Prague, Czech Republic; [5]Department of Pathology 3rd Faculty of Medicine and University Hospital Kralovske Vinohrady, Prague, Czech Republic; [6]The Fingerland Department of Pathology, Charles University, Faculty of Medicine and University Hospital Hradec Kralove, Czech Republic; [7]Department of Gynecology and Obstetrics, Charles University, 3rd Faculty of Medicine and University Hospital Kralovske Vinohrady, Prague, Czech Republic; [8]Gynecologic Oncology Center, Department of Obstetrics and Gynecology, First Faculty of Medicine, Charles University and General University Hospital, Prague

5278

Introduction

Epithelial ovarian carcinoma (EOC) is among the top five causes of cancer-related death in women. Most women with EOC achieve complete remission after primary or interval cytoreductive surgery combined with chemotherapy based on a platinum-taxane doublet. Homologous recombination (HR) defects imposed by germline or somatic BRCA1 DNA repair-associated (*BRCA1*) or *BRCA2* mutations are not only key determinants of platinum sensitivity in EOC patients but also provide a strong rationale for maintenance therapy based on poly(ADP-ribose) polymerase (PARP) inhibitors, which is generally associated with improved progression-free survival (PFS). Besides direct cytotoxic and cytostatic properties, PARPi have been shown to mediate multipronged immunostimulatory effects, largely reflecting their ability to inhibit DNA repair in malignant cells and indicating the possibility to synergy with immune-check point inhibitors (ICIs). Thus, combinatorial regimens involving PARPi and ICIs are emerging as a potential strategy for the management of EOC. Despite recent advances in the clinical evaluation of PARPi and ICIs therapy, the impact of combined therapy on anti-tumor immunity development, spatial contexture and ICI-responsive T cells subsets within tumor-microenvironment is relatively unknown in EOC.

Figure 1

PARPi drive a STING-dependent type I IFN signaling in *Brca1*$^{-/-}$ BR5 as compared to ID8 cell line.

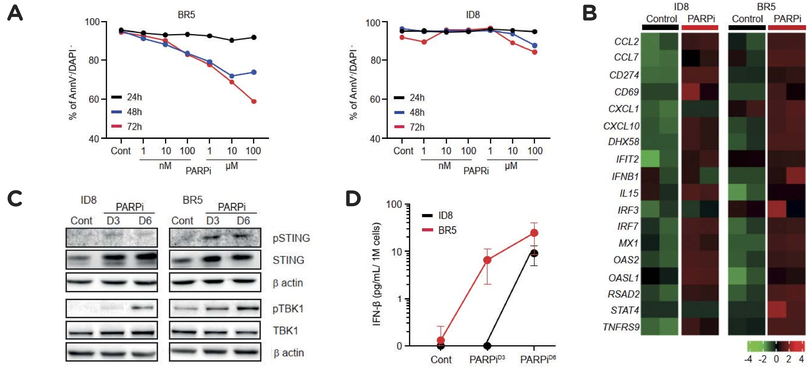

(A) Flow cytometry analyses for frequency of viable AnnV$^-$ and DAPI$^-$ BR5 and ID8 cells after Olaparib (PARPi) at 24, 48 and 72 hours. **(B)** Supervised hierarchical clustering of gene signatures related to type I IFN signaling in control and 1µM Olaparib (PARPi)-treated ID8 and BR5 cell lines as determined by RNA sequencing (RNAseq). **(C)** Phosphorylation of STING and TBK1 in control and Olaparib (PARPi)-treated ID8 and BR5 cell lines at day 3 (D3) and 6 (D6), determined by immunoblotting. **(D)** IFNβ production by ID8 and BR5 cells 24 h after Olaparib (PARPi) therapy, determined by ELISA.

Aim of study

Here we evaluate PARPi immunomodulatory activity, with a specific focus on molecular and cellular pathways that can be harnessed to develop superior combinatorial regimens with ICIs for clinical management of EOC, using multiparametric flow cytometry, multiplex immunostaining, single cells transcriptomics and functional studies in experimental *Brca1*$^{-/-}$ BR5 ovarian syngeneic mouse model.

Figure 2

Figure 2. PARPi elicit STING-dependent anti-tumor immunity in *Brca1*$^{-/-}$ BR5 cell line.

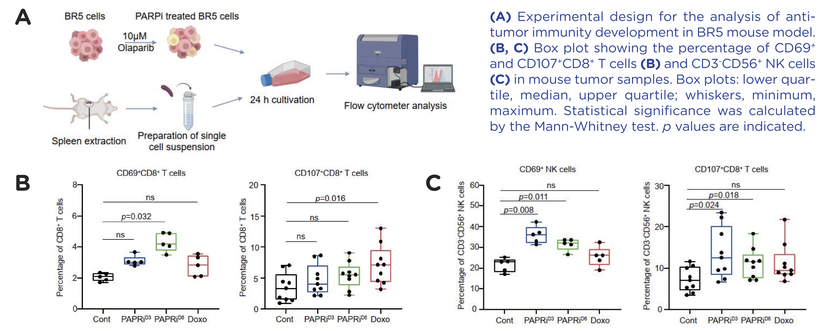

(A) Experimental design for the analysis of anti-tumor immunity development in BR5 mouse model. **(B, C)** Box plot showing the percentage of CD69$^+$ and CD107$^+$CD8$^+$ T cells **(B)** and CD3$^-$CD56$^+$ NK cells **(C)** in mouse tumor samples. Box plots: lower quartile, median, upper quartile; whiskers, minimum, maximum. Statistical significance was calculated by the Mann-Whitney test. *p* values are indicated.

Figure 5

Immunomodulatory properties of combined PARPi and aPD1 therapy. The combination of PARPi and aPD1 positively regulate the balance between adaptive anti-tumor immunity and innate myeloid components and improve the cytotoxic T cell profile in *Brca1*$^{-/-}$ BR5 experimental mouse model.

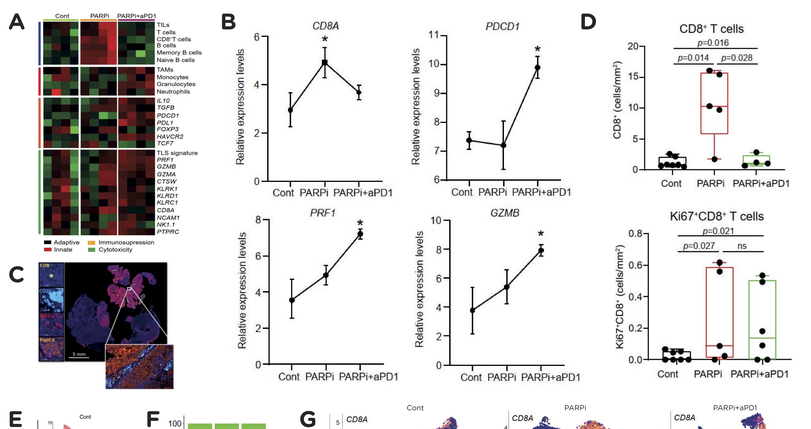

(A) Supervised hierarchical clustering of gene signatures related to adaptive (blue) and innate (red) immunity, immunosuppression (orange) and cytotoxicity (green) and **(B)** gene expression signature associated with CD8$^+$ T cells (determined by MCP counter) and relative gene expression levels of *CD8A*, *GZMB*, *PRF1*, *PDCD1* as determined by RNAseq data in tumor samples of *Brca1*$^{-/-}$ BR5 model after combined PARPi and aPD1 as compared to PARPi alone. **(C)** Representative image of CD8, CD20, Ki67 and PanCK determined by immunostaining. Scale bars 5mm and 10 µm. **(D)** Density of CD8$^+$ T cells and Ki67$^+$ CD8$^+$ T cells in tumor samples of *Brca1*$^{-/-}$ BR5 model after combined PARPi and aPD1 as compared to PARPi alone. **(E)** t-distributed stochastic neighbour embedding (tSNE) analysis of cell that passed quality checks in *Brca1*$^{-/-}$ BR5 tumor after combined PARPi and aPD1 as compared to PARPi alone. Cells and clusters are color coded by the major cell type found. **(F, G)** The distribution of cell types **(F)** and feature plot showing expression of key genes across CD8$^+$ T cell clusters **(G)** between control, PARPi and combined PARPi and aPD1 therapy. Statistical significance was calculated by the Mann-Whitney test. *p* values are indicated.

Figure 3

PARPi in both early and late setting provide survival benefit to *Brca1*$^{-/-}$ BR5 experimental model.

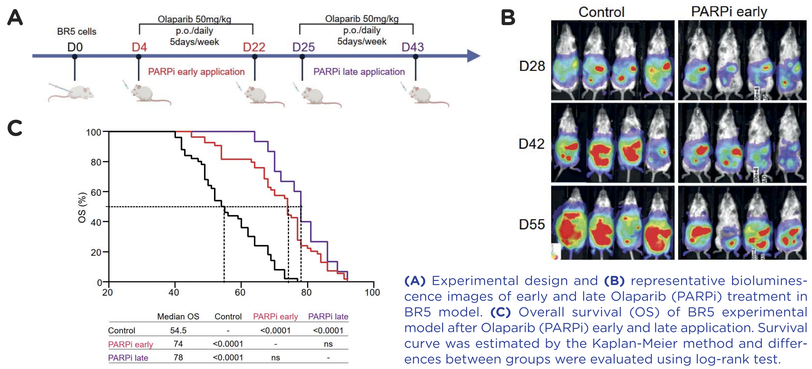

(A) Experimental design and **(B)** representative bioluminescence images of early and late Olaparib (PARPi) treatment in BR5 model. **(C)** Overall survival (OS) of BR5 experimental model after Olaparib (PARPi) early and late application. Survival curve was estimated by the Kaplan-Meier method and differences between groups were evaluated using log-rank test.

Figure 4

PARPi enhance the clinical benefit of ICIs therapy in *Brca1*$^{-/-}$ BR5 experimental model.

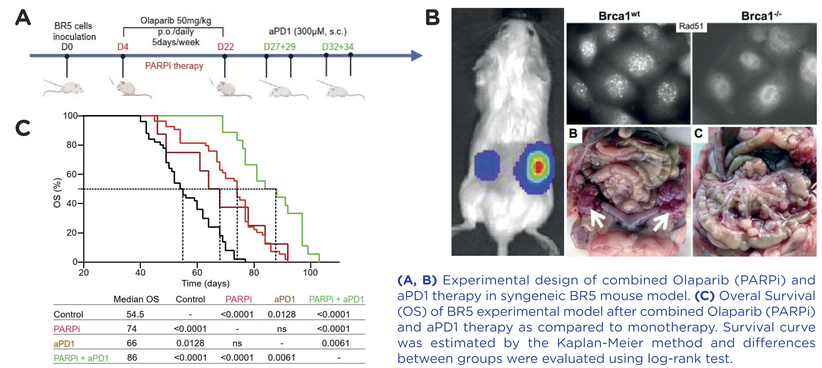

(A, B) Experimental design of combined Olaparib (PARPi) and aPD1 therapy in syngeneic BR5 mouse model. **(C)** Overal Survival (OS) of BR5 experimental model after combined Olaparib (PARPi) and aPD1 therapy as compared to monotherapy. Survival curve was estimated by the Kaplan-Meier method and differences between groups were evaluated using log-rank test.

Conclusions

Our finding demonstrates, that PARPi elicit STING-dependent anti-tumor immunity in *Brca1*$^{-/-}$ BR5 derived experimental model as compared to *BRCA1* proficient ID8 model. Supporting this notion, the combination of PARPi and aPD1 positively regulate the balance between adaptive anti-tumor immunity and innate myeloid components and significantly improve the cytotoxic T cell profile as shown in both experimental mice model. We surmise that rationally designed combinations of PARPi and immunotherapy might be critical to unlock immunosuppression in the EOC microenvironment in support of clinical efficacy.

For more information please contact: holicek@sotio.com, fucikova@sotio.com